Electronic Supplementary Information

Supplementary video

Supplementary video 1. The 3D COMSOL model of PFP-TENG.
Supplementary video 2. The PFP-TENG drives electronic clock for timing task.
Supplementary video 3. The PFP-TENG drives calculator for computing.
Supplementary video 4. The PFP-TENG drives LED array by flapping.
Supplementary video 5. The PFP-TENG drives LED array by trampling.
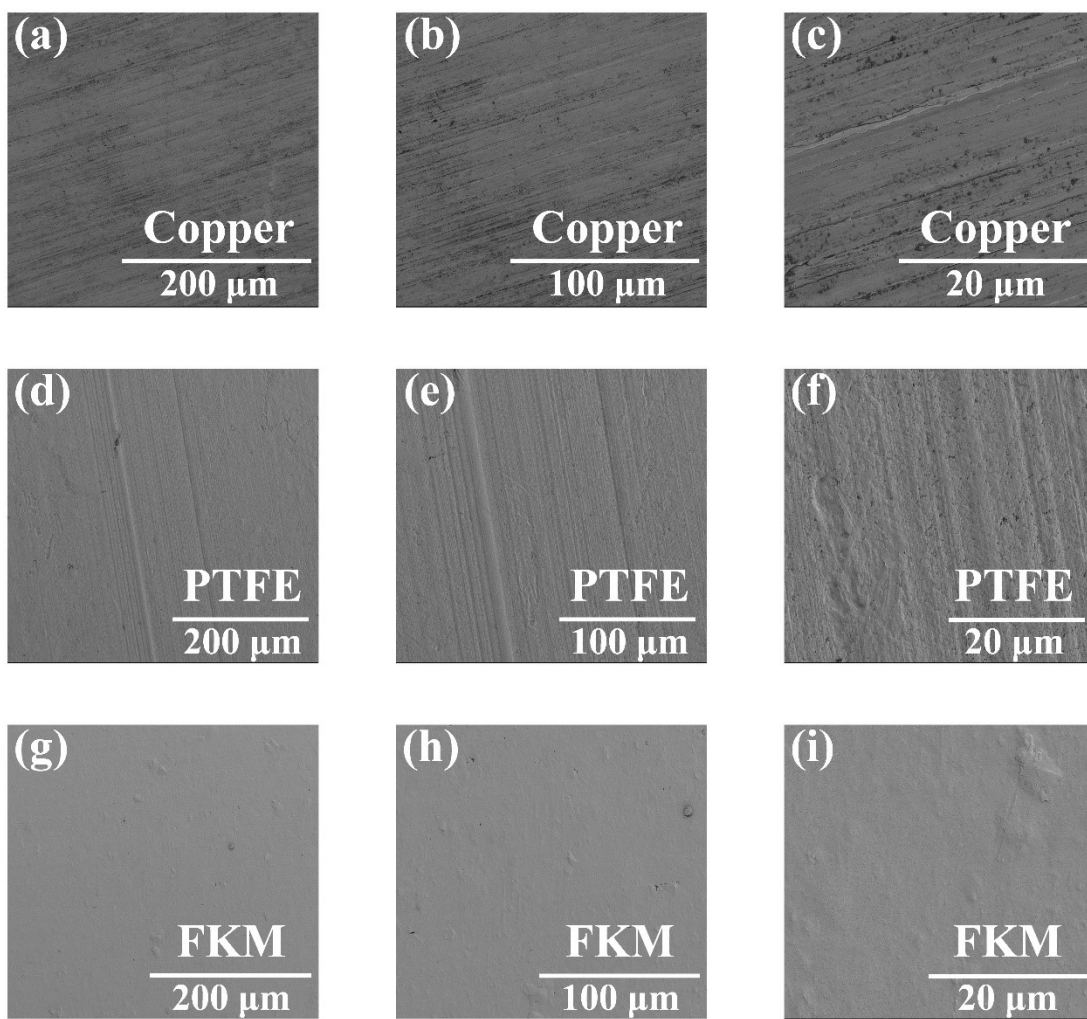**Supplementary video 6.** The PFP-TENG drives LED array by walking.

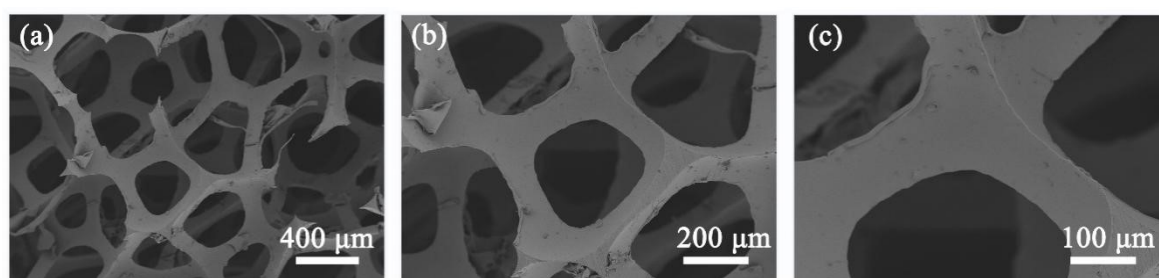**Figure S1**. The SEM of (a-c)Copper, (d-f)PTFE and (g-i)FKM.
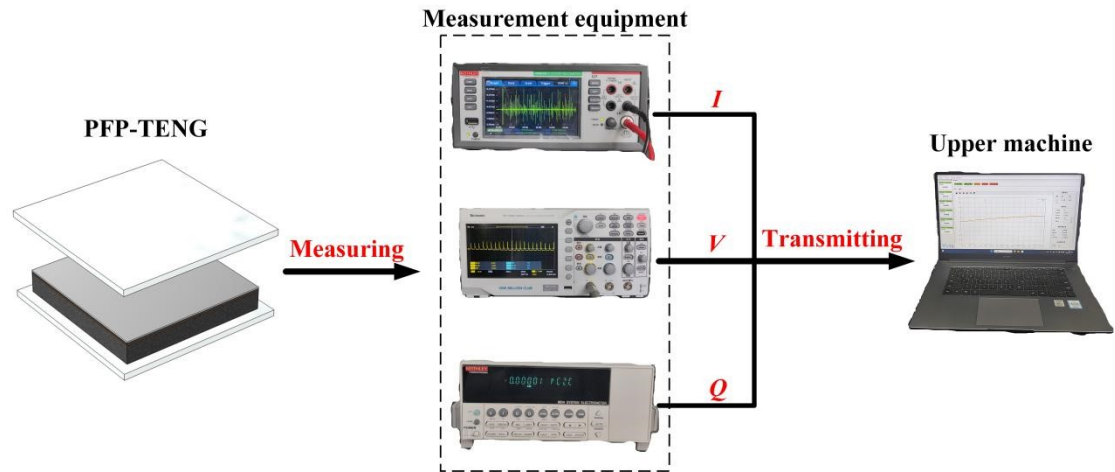

Figure S2 The SEM of (a-c)PU.

Figure S3 The diagram of measurement platform.

The COMSOL simulation of PFP-TENG

The electrostatic field simulation of PFP-TENG is completed by operating COMSOL software in this work. At first, We establish a COMSOL file, set the spatial dimension to three dimensions, and use the electrostatic field for the steady-state study. In **Fig.S5**, a sphere with a radius of 30 cm and an outer edge thickness of 2 cm is built, which is used as the operating space of the TENG. The outer edge is set to an infinite element domain, and the three-dimensional modeling of the PFP-TENG is performed in the central region according to the actual size (as shown in **Fig.S6**). The displacement variable P is introduced into Plate A, and its variable range is 2.3 ~ 2.8. The second step is to select the corresponding materials in the material library and set the attributes of different parts. In addition to the PFP-TENG, the rest are set to air. Then, according to the theoretical model, working principle and actual current output results, the surface charge density of corresponding tribo-layers is set ($\sigma_{PTFE} = 54.42*10^{\wedge}-6[C/m^{\wedge}2]$). The edge of conductive layer is grounded as the boundary condition. Finally, the grid size is set to fine, and the distribution of potential and electric field lines as shown in **Fig. S7** is obtained by parametric scanning.
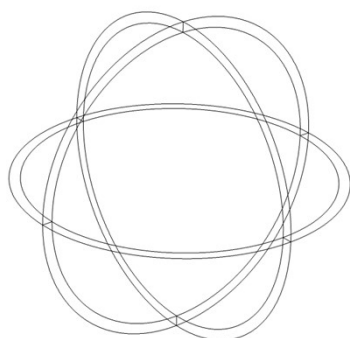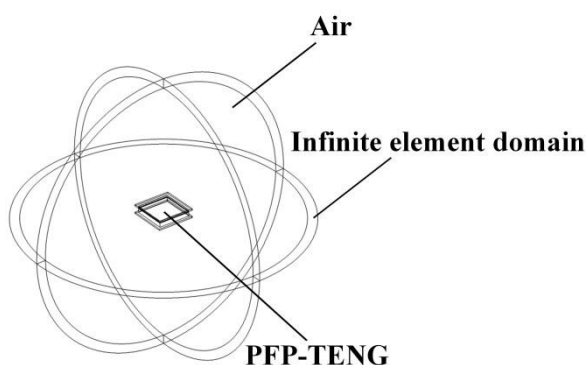

Figure S4 The operating space of PFP-TENG.

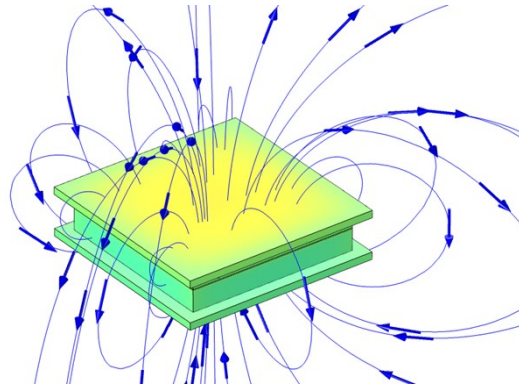**Figure S5** The COMSOL simulation model of PFP-TENG.

Figure S6 The potential and electric field lines distribution of PFP-TENG.

The comparison of theoretical model

By using the Gauss theorem to derive, the relationship can be carried out for the traditional vertical contact-separation mode and the PFP-TENG proposed in this paper.

1.The vertical contact-separation TENG

In **Figure 2(a)**, The electric fields in a general vertical contact-separation TENG can be expressed (Where $x(t)$ is the distance between the contact surfaces, d_1, d_2, ε_{r1}, ε_{r2} correspond to the thickness of the tribo-layers and the relative dielectric constant of the constituent material, respectively.).

In dielectric material 1:

$$E_1 = -\frac{Q_1}{S\varepsilon_0\varepsilon_{r1}} \tag{S1}$$

In the air gap(σ_1 is the surface frictional charge density):

$$E_{air} = \frac{-\frac{Q_1}{S} + \sigma_1}{\varepsilon_0} \tag{S2}$$

In dielectric material 2:

$$E_2 = -\frac{Q_1}{S\varepsilon_0\varepsilon_{r2}} \tag{S3}$$

The potential difference between the two electrodes:

$$V = E_1 d_1 + E_2 d_2 + E_{air}x \tag{S4}$$

Then, the *V-Q-x* relationship of the general dielectric-dielectric TENG model is

$$V = \frac{Q_1}{S\varepsilon_0}(\frac{d_1}{\varepsilon_{r1}} + \frac{d_2}{\varepsilon_{r2}} + x(t)) + \frac{\sigma_1 x(t)}{\varepsilon_0} \tag{S5}$$

Therefore, the output performance (V_{OC}, Q_{SC}, and C) of this basic mode TENG can be shown as:

$$\begin{cases} V_{OC} = \dfrac{\sigma_1 x(t)}{\varepsilon_0} \\[4mm] Q_{SC} = \dfrac{\varepsilon_{r1}\varepsilon_{r2}S\sigma_1 x(t)}{\varepsilon_{r2}d_1 + \varepsilon_{r1}d_2 + \varepsilon_{r1}\varepsilon_{r2}x(t)} \\[4mm] C = \dfrac{\varepsilon_{r1}\varepsilon_{r2}\varepsilon_0 S}{\varepsilon_{r2}d_1 + \varepsilon_{r1}d_2 + \varepsilon_{r1}\varepsilon_{r2}x(t)} \end{cases} \tag{S6}$$

2.PFP-TENG

It is worth noting that in the model of PFP-TENG, attributing to the corporation of Electrode 1 and FKM, the PTFE layer shows more triboelectric charge ($-S\sigma_2=-Q_2$). However, due to the smaller air gap between PTFE and FKM, the FKM can only present less positive charge, which can be expressed as $Q_2-S\sigma_c$. In addition, the design of the PFP-TENG also introduces an electropositive PU sponge, which can not only bring a better bonding effect between the interfaces, but also induce some positive charges during compression deformation, maintain the electrical equilibrium, and promote the generation of induced current in the external circuit.

In **Figure 2(b)**, The electric fields in PFP-TENG can be expressed to:

$$\begin{cases} E_1 = -\dfrac{Q_2}{S\varepsilon_0\varepsilon_{r1}} \\[2em] E_{air} = \dfrac{-\dfrac{Q_2}{S}+\sigma_2}{\varepsilon_0} \\[2em] E_2 = -\dfrac{Q_2-S\sigma_c}{S\varepsilon_0\varepsilon_{r1}} \end{cases} \tag{S7}$$

According to the potential difference between the two electrodes, the V-Q-x relationship of PFP-TENG is concluded as follows:

$$V = -\frac{Q}{S\varepsilon_0}(\frac{d_1}{\varepsilon_{r1}}+\frac{d_2}{\varepsilon_{r2}}+x(t))+\frac{\sigma_2 x(t)}{\varepsilon_0}+\frac{\sigma_c d_2}{\varepsilon_0\varepsilon_{r2}} \tag{S8}$$

Finally, the corresponding output performance can also be derived:

$$\begin{cases} V_{OC} = \dfrac{\varepsilon_{r2}\sigma_2 x(t)+\sigma_c d_2}{\varepsilon_0\varepsilon_{r2}} \\[2em] Q_{SC} = \dfrac{(\varepsilon_{r2}\sigma_2 x(t)+\sigma_c d_2)S\varepsilon_{r1}}{\varepsilon_{r2}d_1+\varepsilon_{r1}d_2+\varepsilon_{r1}\varepsilon_{r2}x(t)} \\[2em] C = \dfrac{S\varepsilon_0\varepsilon_{r1}\varepsilon_{r2}}{\varepsilon_{r2}d_1+\varepsilon_{r1}d_2+\varepsilon_{r1}\varepsilon_{r2}x(t)} \end{cases} \tag{S9}$$

From the comparison of the above two theoretical TENG models, it is clear to see that the PFP-TENG with stacked structure have better performance in output voltage and transferred charge. Due to the higher frictional charge density on the surface, the special charge balance state in the stacked structure and the support of the elastomer, the conductive layer on the two plates can produce more induced charges and improve the energy conversion efficiency of the power generation device.
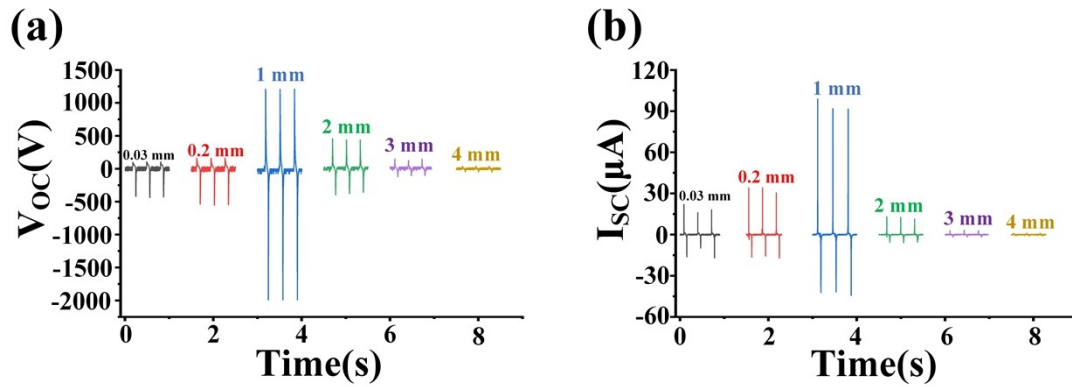
Figure S7 The (a)V_{OC} and (b)I_{SC} at different thicknesses of PTFE.
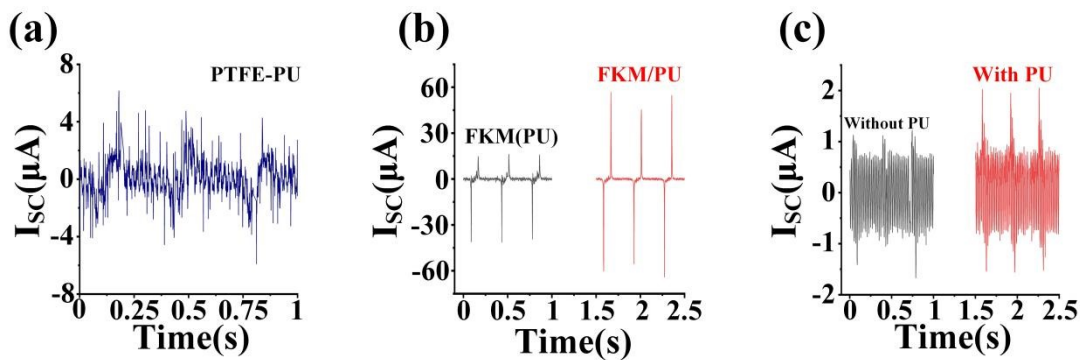

Figure S8 The I_{SC} of (a) the PTFE-PU TENG. The comparison of (b)PTFE-FKM TENG with PU substrate and the stacked FKM/PU TENG. (c)The effect of PU.

The PU sponge plays a significant role in the PFP-TENG proposed in this paper. It must be emphasized that before the following discussion, the compression degree of PU reached its maximum in this part. In **Fig. S8a**, due to the weak triboelectric properties, the maximum I_{SC} of the PU-TENG composed is less than 8 μA, and the output performance is low. In **Fig. S8b**, when the PU is used as the substrate of the FKM-TENG (isolating the contact between PU and the conductive layer), this only brings elastic deformation to the TENG and does not promote the generation of more induced charges. The output has not been distinctly improved. However, when the PU is stacked on the conductive layer, the comprehensive performance is almost improved by 35 %. This should be due to the optimized interface contact effect and the extension of the bonding time. At the same time, the PU layer induces more charges in the conductive copper during the elastic deformation process. This coupling characteristic even achieves the effect of exceeding the sum of the two dielectric-dielectric triboelectric nanogenerators (The FKM-TENG and PU-TENG). In addition, in extreme cases, the effect of PU is still very obvious. As **Fig.S8c**, the same material PTFE is used to contact the PFP-TENG (to isolate the triboelectric effect of the contact surface). It is not difficult to see that the presence or absence of PU layer has a huge influence on the TENG. After adding PU, even without an

effective triboelectric excitation, the PFP-TENG can still generate a small output during the compression process.
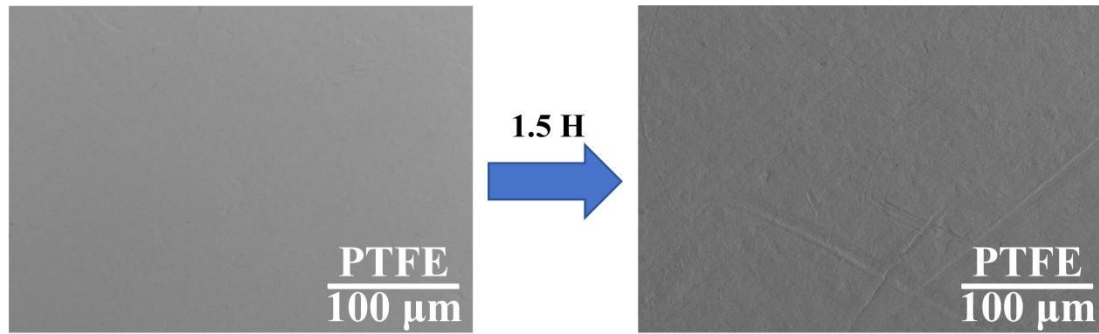

Figure S9 The SEM of PTFE after the durability experiment.